Available online at www.sciencedirect.com
ScienceDirect
International Journal of Solids and Structures 45 (2008) 320–335
INTERNATIONAL JOURNAL OF SOLIDS AND STRUCTURES
www.elsevier.com/locate/ijsolstr

Shape memory elastic foundation and supports for passive vibration control of composite plates

Victor Birman *

University of Missouri-Rolla, Engineering Education Center, One University Boulevard, St. Louis, MO 63121, USA

Received 3 December 2006; received in revised form 20 June 2007
Available online 12 September 2007

Abstract

The paper presents an approach to passive vibration control of shear deformable and thin plates. The first of two methods of vibration control employs prestressed shape memory alloy (SMA) wires embedded in sleeves attached to the surface of the plate. The spacing between the wires can be arbitrary and variable enabling the development of a SMA support system for maximum control with minimum additional weight. The other method considered in the paper utilizes SMA wires supporting the plate at strategically selected points. The mechanism of passive control includes two components: (1) SMA wires prestressed as a result of constrained phase transformation act as an elastic foundation with a variable stiffness and (2) energy dissipation occurs as a result of hysteresis in superelastic wires vibrating together with the structure. As follows from examples, it is possible to achieve a significant reduction of the vibration amplitude over a broad spectrum of driving frequencies using any of two methods considered in the paper.

Keywords: Shape memory alloy; Vibration control; Composite plates

1. Introduction

Shape memory alloy (SMA) elements have been considered for control of vibrations as well as for the enhancement of stability of composite and metallic plates by numerous investigators. The early work in this direction was reviewed by the author (Birman, 1997a). In general, a reduction of vibration amplitudes using SMA can be achieved through two mechanisms. SMA fibers or wires prestressed through a phase transformation apply tensile forces to the structure increasing its effective stiffness. If SMA elements operate in the superelastic regime, significant energy dissipation reflected in a large hysteresis loop also results in a reduction of dynamic deformations.

The method used to reduce dynamic response or enhance stability is often based on embedding SMA fibers within the structure. Some of the studies concerned with embedding SMA fibers bonded to the composite substrate are referred to in the paper of Birman (1997a); a comprehensive review of this subject is outside the scope

* Tel.: +1 314 516 5431; fax: +1 314 516 5434.
E-mail address: vbirman@umr.edu

0020-7683/$ - see front matter
doi:10.1016/j.ijsolstr.2007.08.023

of this paper. Investigations of the effect of SMA wires embedded in sleeves preventing direct contact between SMA and the substrate were initiated by Baz and his collaborators. For example, multiple dynamic problems of composite structures reinforced with such wires in sleeves were considered by Baz et al. (1995) and Ro and Baz (1995). Embedding SMA wires in sleeves provides a number of advantages, including an ease of activation and a reduction of the effect of temperature changes in the wire on the adjacent composite structure. A further improvement can be achieved by placing the sleeves outside the structure, i.e. bonding them to the surface, rather than embedding within the structure (Epps and Chandra, 1997). SMA wires in sleeves that are externally bonded to the structure serve as an equivalent elastic foundation resisting deflections of the structure.

The dissipation of energy in a superelastic SMA wire also results in a reduction of the dynamic response (Thomson et al., 1995; Ip, 2000; Zhang et al., 2003). The area of the hysteresis loop of SMA is large but the complete hysteresis can be achieved only if the range of strains reaches several percents. Although such large range of strain is unlikely in plates and shells, dampers utilizing the complete superelastic hysteresis have been considered for civil engineering applications (Saadat et al., 2002; Seelecke et al., 2002) and in spring-mass isolation systems (Lagoudas et al., 2004). In the present problem, superelastic wires undergo an incomplete hysteresis (inner or internal hysteresis loop). Accordingly, the dissipation of energy may be a secondary effect in the control of forced vibrations compared to the resistance of stretched wires to deflections of the structure. Nevertheless, the following solution accounts for both phenomena since the contribution of hysteretic damping may become dominant if the driving frequency is close to the resonant frequency of the structure with prestressed SMA wires (detailed discussion of this subject is presented below in Section 3.1).

It should be noted that SMA wires represent an alternative to prestressed steel wires. One of the advantages of SMA wires is related to the possibility to activate them on the "as needed" basis. Accordingly, the recovery force is applied by such wire to boundary structures only when the supported structure is subject to external loads whose action should be compensated. In the contrary, a prestressed steel wire should be maintained in the "active" state throughout the life of the structure. In addition, it is noted that it is possible to activate a SMA wire by raising temperature below the austenite finish value achieving a partial phase transformation. This feature may provide certain flexibility related to "shifting" the natural frequencies of the SMA-reinforced structure away from the driving frequency.

The solution presented in the paper refers to a shear deformable composite plate analyzed by a first-order theory. The particular case of a thin plate treated by the classical plate theory is also presented.

2. Analysis

Consider a shear deformable rectangular plate with SMA wires in sleeves bonded to one of the surfaces as shown in Fig. 1. SMA wires can freely slide along the sleeves, i.e. friction is negligible. One of the advantages of such design compared to embedding SMA fibers in sleeves within the structure is related to the ease of manufacture. In addition, external sleeves do not compromise the integrity of the composite structure as may

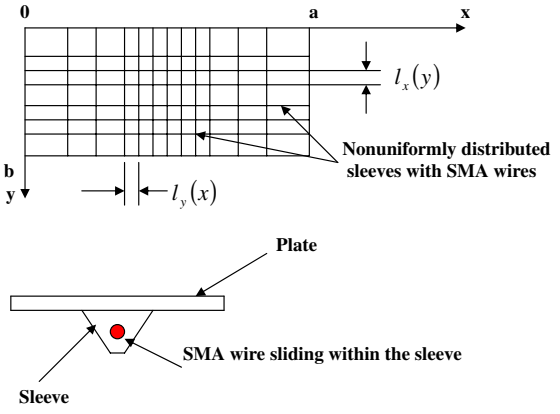

Fig. 1. SMA wires in sleeves bonded with a variable spacing providing a larger support at the central part of the plate. A detail of the cross section with a SMA wire that is free to slide along the sleeve is also shown.

be the case if they were embedded. The issues of maintenance and joining SMA wires to supports are also easier solved in the configuration considered here. It is assumed that the stiffness of the sleeve material is small, i.e. the sleeves do not affect the matrix of stiffnesses of the plate. If necessary, this requirement can be enforced by cutting the sleeves at periodic, closely spaced intervals. In the unlikely case where it is necessary to account for the contribution of the sleeves, their stiffness can be incorporated in the analysis using either the standard discrete stiffener approach or the smeared stiffeners technique if the spacing between the sleeves is small (Birman, 1997b). The contribution of the sleeves and SMA wires to the inertial coefficients is included in the present solution.

Prior to the installation, a SMA wire is cooled so that the material is transformed into martensite and stretched to a required length. Subsequently, it is inserted in the sleeves and constrained by joining it to the supporting structure. As temperature returns to the operational level corresponding to the austenitic phase of SMA, the wire is in tension as a result of constrained recovery, while the supporting structure resists the reactive forces. Such approach has been introduced and applied in numerous studies; some of them are referred to in Introduction. As is shown in Fig. 1, two mutually perpendicular systems of wires oriented along the edges of the plate overlap. Several methods of design of such overlapping systems could be suggested but these details are outside the scope of this paper (of course, desirable results could also be achieved using a single system of wires oriented along either x or y directions).

As was shown by Epps and Chandra (1997) on the example of a beam, the effect of a stretched wire that can freely slide within the sleeve continuously bonded to the vibrating structure is equivalent to that of an elastic foundation with the stiffness varying along the axis of the wire. In the present paper, we formulate the problem of an optimal distribution of SMA wires bonded to the plate either continuously or at selected points with the goal of reducing the dynamic response to a prescribed level. The approach considered in the paper provides the following advantages:

1. Optimizing the distribution of SMA wires (or attaching the sleeves to the plate at appropriately selected points) it is possible to minimize the number of wires and maximize their effectiveness, while reducing the reactive force that is applied to the supporting structure.
2. The wires located in the sleeves outside the body of the plate can be activated thermally on the "as needed" basis, without significant heat transfer to the plate. Accordingly, the reactive force applied to the supporting structure will be generated only during time intervals when the plate experiences significant vibrations.

As is noted above, the amplitude of forced vibrations of the plate is reduced due to two mechanisms:

1. The "elastic foundation" or "elastic supports" provided by stretched SMA wires;
2. Superelastic hysteresis in a SMA wire when it experiences vibrations. The strain range of a typical vibrating structure being relatively small compared to the range needed for a complete hysteresis loop in such SMA as Nitinol, it is anticipated that the wire experiences an incomplete hysteresis.

2.1. SMA wires in sleeves continuously bonded to the plate

The plate considered in the analysis is assumed symmetric about its middle plane. Accordingly, the equations of motion can be obtained as an extension of the equations for a shear deformable plate without an elastic foundation presented in numerous references, such as the monograph of Reddy (2004):

$$\begin{aligned}
&A_{55}(w_{,xx}+\phi_{x,x})+A_{44}(w_{,yy}+\phi_{y,y})-[k_1(x,y)+k_2(x,y)]w+q(x,y,t)=m(x,y)\ddot{w}+[c_1(x)+c_2(y)]\dot{w}\\
&D_{11}\phi_{x,xx}+D_{66}\phi_{x,yy}+(D_{12}+D_{66})\phi_{y,xy}-A_{55}(w_{,x}+\phi_x)=I(x,y)\ddot{\phi}_x\\
&D_{22}\phi_{y,yy}+D_{66}\phi_{y,xx}+(D_{12}+D_{66})\phi_{x,xy}-A_{44}(w_{,y}+\phi_y)=I(x,y)\ddot{\phi}_y
\end{aligned} \tag{1}$$

where w is a dynamic deflection, ϕ_x, ϕ_y are rotations of the normal to the plate surface, the extensional (A_{ij}) and bending (D_{ij}) stiffness coefficients are defined in the customary manner and q is the applied dynamic pressure. The stiffness terms A_{44}, A_{55} incorporate the shear correction factor. The stiffness of the equivalent elastic foundation produced by the systems of wires oriented in the y and x directions are denoted by

$k_1(x,y)$ and $k_2(x,y)$, respectively, while $c_1(x)$, $c_2(y)$ are equivalent viscous damping coefficients of the corresponding systems of wires. The derivation of $k_1(x,y)$, $k_2(x,y)$ and $c_1(x)$, $c_2(y)$ is shown below.

The transverse inertial term includes the mass per unit surface area of the plate that can be calculated accounting for the weight of sleeves and wires and using the analogy to the smeared stiffeners technique:

$$m(x,y) = \rho_p h + \frac{\rho_w A_y + \rho_s A_{sy}}{l_y} + \frac{\rho_w A_x + \rho_s A_{sx}}{l_x}, \tag{2}$$

where ρ_p, ρ_w and ρ_s denote the mass density of the plate, wire and sleeve materials, respectively, h is the thickness of the plate, and $l_y = l_y(x)$ and $l_x = l_x(y)$ are spacings of the systems of wires oriented in the y and x directions, respectively. The cross sectional areas of the wires oriented in the y and x directions and the cross sectional areas of the sleeves encompassing these wires are denoted by A_y, A_x, A_{sy} and A_{sx}, respectively.

The rotational inertia can also be evaluated "smearing" the wires in sleeves over the surface of the plate, so that

$$I(x,y) = \int \rho_p z^2 \, dz + \frac{\rho_w I_y + \rho_s I_{sy}}{l_y} + \frac{\rho_w I_x + \rho_s I_{sx}}{l_x}. \tag{3}$$

In (3), the integration is conducted through the thickness of the plate, while I_y, I_{sy}, I_x, I_{sx} denote the moments of inertia of respective wires and sleeves oriented in the y and x directions about the middle plane of the plate.

The damping coefficient of a system of wires can be determined in terms of the coefficient of a single wire C_w. Then the smeared damping produced by the systems of wires oriented in the y and x directions is

$$c_1 = \frac{C_{wy}}{l_y} \quad c_2 = \frac{C_{wx}}{l_x}, \tag{4}$$

where C_{wy} and C_{wx} represent damping produced in a single wire oriented in the y and x directions, respectively.

In the areas of the plate where the distance between the wires is large smearing the inertial and damping effects may become inaccurate so that each wire has to be accounted for individually. This can be accomplished by replacing the spacing in (2)–(4) with a Dirac delta function, so that $\frac{1}{l_x} \to \delta(y - y_j)$, $\frac{1}{l_y} \to \delta(x - x_i)$, x_i and y_j being the coordinates of the corresponding wire.

The stiffness of the foundation modeling the effect of a system of wires is now derived expanding the solution for a single wire by Epps and Chandra (1997). The bending stiffness of the wire could be accounted for but it is negligible in realistic design applications. The bending moment acting at a cross section $x = \xi$ of a wire oriented in the x-direction, stretched by a tensile force T and subject to a concentrated force Q as shown in Fig. 2 is

$$M = \frac{Q(a-\xi)}{a}x - Tw - [Q(x-\xi)]_{x \geqslant \xi}. \tag{5}$$

The negligible bending stiffness of the wire implies that this moment is equal to zero. Accordingly, the deflection of the wire at the point of application of the force is

$$w(x = \xi) = \frac{Q(a-\xi)\xi}{Ta}. \tag{6}$$

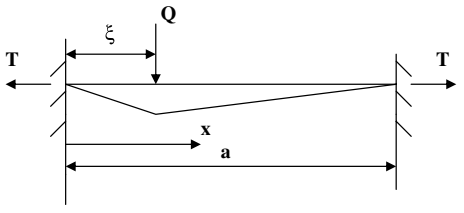

Fig. 2. SMA wire subject to a concentrated force Q at $x = \xi$.

The stiffness of the foundation produced by a system of closely-spaced wires oriented in the x-direction is now available using the smearing technique:

$$k_2(x,y) = \frac{Q}{w(x=\xi)l_y a} = \frac{T}{(a-x)xl_y}. \tag{7}$$

By analogy,

$$k_1(x,y) = \frac{T}{(b-y)yl_x}. \tag{8}$$

In the regions of the plate with sparsely located wires, the corresponding stiffness terms can be adjusted replacing the spacing with the Dirac delta function as explained above. The evaluation of damping in a wire as a result of incomplete superelastic hysteresis is discussed in Section 2.2.

It is noted that the recovery force in SMA wires does not remain constant during the motion. Vibrations of wires result in small-amplitude axial displacements and accordingly, dynamic components superimposed on the static force T. However, in a linear problem, such dynamic components remain negligible compared to a large static recovery force in the wire.

Note that for practical manufacturing reasons it may be convenient to cut the sleeves at some distance from the boundaries supporting only the central section of the plate where vibrations are maximum. In this case the boundaries of the region of the plate supported by prestressed wires are $a_1 < x < a_2$, $b_1 < y < b_2$ as reflected in Fig. 3. The correction to the inertial term can be disregarded, if the supported region is extended close to the edges of the plate.

The elastic foundation provided by SMA wires does not affect the boundary conditions of the plate. Accordingly, if the edges of the plate are supported by stringers that posses infinite bending and axial stiffness and a negligible torsional stiffness, the corresponding conditions are

$$\begin{aligned} &x = 0, \quad x = a: \\ &w = 0, \quad \phi_y = 0, \quad M_x = D_{11}(w_{,xx} + \phi_{x,x}) + D_{12}(w_{,yy} + \phi_{y,y}) = 0 \\ &y = 0, \quad y = b: \\ &w = 0, \quad \phi_x = 0, \quad M_y = D_{12}(w_{,xx} + \phi_{x,x}) + D_{22}(w_{,yy} + \phi_{y,y}) = 0. \end{aligned} \tag{9}$$

It is evident that conditions (9) are identically satisfied by the solution in the form

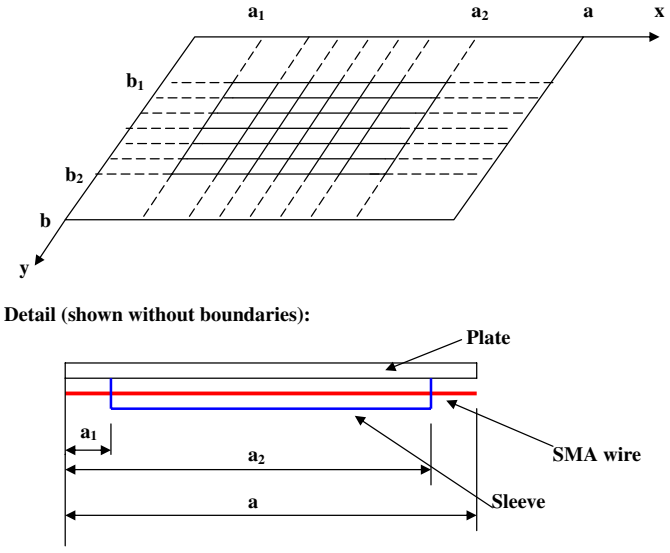

Fig. 3. Plate supported by SMA wires in sleeves within the region $a_1 < x < a_2$, $b_1 < y < b_2$. Solid lines identify wires in the region of the plate supported by the sleeves. Dashed lines are wires in the unsupported regions.

$$
\begin{aligned}
w &= \sum_{m,n} W_{mn}(t)\,\sin\frac{m\pi x}{a}\sin\frac{n\pi y}{b}\\
\phi_x &= \sum_{m,n} H_{mn}(t)\,\cos\frac{m\pi x}{a}\sin\frac{n\pi y}{b}\\
\phi_y &= \sum_{m,n} R_{mn}(t)\,\sin\frac{m\pi x}{a}\cos\frac{n\pi y}{b}.
\end{aligned}
\tag{10}
$$

The substitution of (10) into (1) where the applied pressure of frequency ω is represented by $q=\sum_{m,n}q_{mn}\sin\frac{m\pi x}{a}\sin\frac{n\pi y}{b}\sin\omega t$ and the application of the Galerkin procedure yields a system of coupled algebraic equations with respect to the amplitudes of the terms in series (10):

$$
\begin{aligned}
&\sum_{r,s}\begin{bmatrix} M_{rsmn} & 0 & 0\\ 0 & I^{(1)}_{rsmn} & 0\\ 0 & 0 & I^{(2)}_{rsmn}\end{bmatrix}\begin{Bmatrix}\ddot{W}_{rs}\\ \ddot{H}_{rs}\\ \ddot{R}_{rs}\end{Bmatrix}+\sum_{r,s}\begin{bmatrix} C_{rsmn} & 0 & 0\\ 0 & 0 & 0\\ 0 & 0 & 0\end{bmatrix}\begin{Bmatrix}\dot{W}_{rs}\\ \dot{H}_{rs}\\ \dot{R}_{rs}\end{Bmatrix}+\sum_{r,s}\begin{bmatrix} K_{rsmn} & 0 & 0\\ 0 & 0 & 0\\ 0 & 0 & 0\end{bmatrix}\begin{Bmatrix} W_{rs}\\ H_{rs}\\ R_{rs}\end{Bmatrix}\\
&+\begin{bmatrix} F^{(11)}_{mn} & F^{(12)}_{mn} & F^{(13)}_{mn}\\ F^{(12)}_{mn} & F^{(22)}_{mn} & F^{(23)}_{mn}\\ F^{(13)}_{mn} & F^{(23)}_{mn} & F^{(33)}_{mn}\end{bmatrix}\begin{Bmatrix} W_{mn}\\ H_{mn}\\ R_{mn}\end{Bmatrix}=\sum_{rs}\begin{Bmatrix} q_{rsmn}(t)\\ 0\\ 0\end{Bmatrix},
\end{aligned}
\tag{11}
$$

where the coefficients are

$$
\begin{aligned}
M_{rsmn} &= \frac{4}{ab}\int_0^a\int_0^b m(x,y)S_{rm}(x)S_{sn}(y)\,\mathrm{d}y\,\mathrm{d}x\\
I^{(1)}_{rsmn} &= \frac{4}{ab}\int_0^a\int_0^b I(x,y)C_{rm}(x)S_{sn}(y)\,\mathrm{d}y\,\mathrm{d}x\\
I^{(2)}_{rsmn} &= \frac{4}{ab}\int_0^a\int_0^b I(x,y)S_{rm}(x)C_{sn}(y)\,\mathrm{d}y\,\mathrm{d}x\\
C_{rsmn} &= \frac{4}{ab}\int_{a_1}^{a_2}\int_{b_1}^{b_2}[c_1(x)+c_2(y)]S_{rm}(x)S_{sn}(y)\,\mathrm{d}y\,\mathrm{d}x\\
K_{rsmn} &= \frac{4}{ab}\int_{a_1}^{a_2}\int_{b_1}^{b_2}[k_1(x,y)+k_2(x,y)]S_{rm}(x)S_{sn}(y)\,\mathrm{d}y\,\mathrm{d}x\\
q_{rsmn}(y) &= \frac{4}{ab}\int_0^a\int_0^b q(x,y,t)S_{rm}(x)S_{sn}(y)\,\mathrm{d}y\,\mathrm{d}x\\
F^{(11)}_{mn} &= A_{55}\left(\frac{m\pi}{a}\right)^2+A_{44}\left(\frac{n\pi}{b}\right)^2\\
F^{(12)}_{mn} &= A_{55}\frac{m\pi}{a}\\
F^{(13)}_{mn} &= A_{44}\frac{n\pi}{b}\\
F^{(22)}_{mn} &= D_{11}\left(\frac{m\pi}{a}\right)^2+D_{66}\left(\frac{n\pi}{b}\right)^2\\
F^{(23)}_{mn} &= (D_{12}+D_{66})\frac{m\pi}{a}\frac{n\pi}{b}\\
F^{(33)}_{mn} &= D_{66}\left(\frac{m\pi}{a}\right)^2+D_{22}\left(\frac{n\pi}{b}\right)^2.
\end{aligned}
\tag{12}
$$

In (12),

$$
\begin{aligned}
S_{rm}(x) &= \sin\frac{r\pi x}{a}\sin\frac{m\pi x}{a}\\
C_{rm}(x) &= \cos\frac{r\pi x}{a}\cos\frac{m\pi x}{a}.
\end{aligned}
\tag{13}
$$

Other similar functions are defined by analogy with those in (13); if x is replaced with y, a should be replaced with b.

The integrals that appear in (12), including K_{rsmn}, can be evaluated using a symbolic math program, such as Mathematica. In case where the frequency of the driving pressure is close to the fundamental frequency of the plate so that the analysis can adequately be conducted using a one-degree of freedom approximation, the integrals K_{rsmn} are evaluated in terms of sine and cosine integral functions. For example, if $r = m = 1$ and the sleeves oriented in the x-direction are bonded to the plate within the region $a_1 \leqslant x \leqslant a_2$,

$$\int_{a_1}^{a_2} k_2(x,y) S_{rm}(x)\,\mathrm{d}x = \frac{Ta}{l_y}\int_{a_1}^{a_2} \frac{\sin^2\frac{\pi x}{a}}{(a-x)x}\,\mathrm{d}x$$
$$= \frac{Ta}{l_y}\left\{\frac{\log a_2 - \log a_1}{2a} - \frac{\log(a_2-a)-\log(a_1-a)}{2a} - \frac{1}{2a}\left[Ci\left(\frac{2\pi a_2}{a}\right) - Ci\left(\frac{2\pi a_1}{a}\right) + Ci\left(\frac{2\pi a_2}{a} - 2\pi\right) - Ci\left(\frac{2\pi a_1}{a} - 2\pi\right)\right]\right\}. \quad (14)$$

The evaluation of integrals C_{rsmn} does not present difficulties if the equivalent damping is determined as shown in Section 2.2. Other integrals in (12) can also be calculated.

A relatively simple approximate solution can be obtained by the Rayleigh–Ritz method. Such solution may lead to approximate expressions for the amplitudes of motion that are convenient for a qualitative analysis of the effect of SMA wires. An example of the Rayleigh–Ritz solution for an isotropic beam supported by a system of wires oriented in the axial direction is shown in the Appendix.

2.2. Equivalent viscous damping for a SMA wire

The equivalent viscous damping of a system of SMA wires reflects the dissipation of energy due to a complete or partial phase transformation of the wire material during vibrations. Note that a typical strain range corresponding to the complete hysteresis is of an order of several percent (Seelecke et al., 2002; Zak et al., 2003), i.e. it requires the motion with exceedingly large amplitudes that are not encountered in structural applications involving composite plates. Therefore, it is anticipated that the wire will experience a partial transformation during vibrations corresponding to the range of strain $2\Delta\varepsilon$ as shown in Fig. 4.

A wire in the sleeve that is continuously bonded to the plate is shown in Fig. 3. This section illustrates the computation of damping produced by a system of wires parallel to the y-axis, i.e. $c_1(x)$; the contribution to damping of wires oriented in the x-direction is found through the analogous procedure.

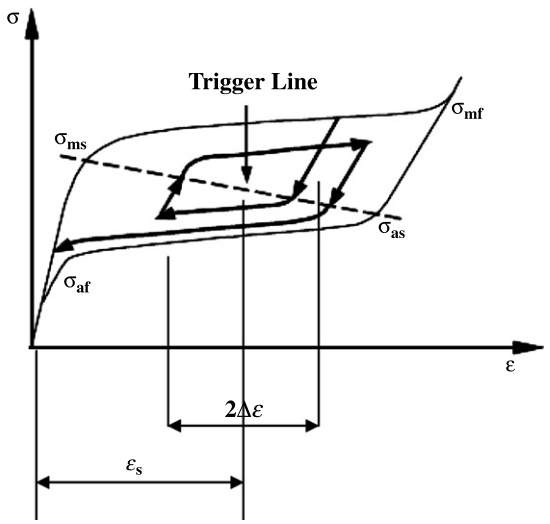

Fig. 4. Dissipation of energy in a prestressed SMA wire vibrating with a prescribed strain range (the corresponding inner hysteresis loop is identified). The range of strains being prescribed, the area of the loop (energy dissipated during the cycle of motion) remains stable during oscillations. Modified figure from Saadat et al. (2002).

The process described here is iterational, i.e. the deflections of the vibrating plate are assumed known from the previous iteration. In the first iteration it is possible to determine deflections from the solution neglecting the effect of damping. At any iteration the motion of a wire located at $x = \bar{x}$ is given by $w = \sum_{m,n} W_{mn}(t) \sin \frac{m\pi\bar{x}}{a} \sin \frac{n\pi y}{b}$. The energy dissipated in the wire during the cycle can be evaluated from the incomplete superelastic hysteresis loop (inner loop) similar to that shown in Fig. 4 using the range of strain specified in the previous iteration. This range is immediately available from

$$2\Delta\varepsilon = 2\left[\frac{1}{2b}\int_0^b w_{\max}(\bar{x},y)_{,y}^2 \,\mathrm{d}y\right] = \frac{1}{2}\sum_n \sum_m \sum_i \left(\frac{n\pi}{b}\right)^2 W'_{mn} W'_{in} \sin\frac{m\pi\bar{x}}{a} \sin\frac{i\pi\bar{x}}{a}, \tag{15}$$

where the prime identifies the amplitude values of the corresponding terms obtained in the previous iteration.

Given static tension in the wire, the pre-strain ε_s is immediately available. Subsequently, the area enclosed within the inner hysteresis loop limited by the strains $\varepsilon_{\max} = \varepsilon_s + \Delta\varepsilon$, $\varepsilon_{\min} = \varepsilon_s - \Delta\varepsilon$ can be found as

$$\Delta U_d = \int_{V_w} \oint_{\varepsilon} \sigma(\varepsilon)\,\mathrm{d}\varepsilon\,\mathrm{d}V_w, \tag{16}$$

where the integration is conducted over the volume of wire V_w. This area represents the amount of energy dissipated in the wire during a cycle of motion. Note that a relatively simple method of calculation of energy dissipated during a cycle of motion corresponding to an incomplete transformation based on the complex modulus approach was suggested by Gandi and Wolons (1999). The model of Masuda and Noori (2002) can also be used to evaluate the dissipated energy corresponding to the inner hysteresis loop.

Let the wire be replaced with a uniaxial continuous equivalent viscous damper with the damping coefficient C_{wy}. The energy dissipated in such damper during one cycle of motion would be (Soedel, 1993)

$$\Delta U'_d = \frac{1}{2}\int_0^{2\pi/\omega}\int_0^b C_{wy}\dot{w}^2(\bar{x},y)\,\mathrm{d}y\,\mathrm{d}t = \frac{b}{4}C_{wy}\int_0^{2\pi/\omega}\sum_{m,n}\sum_{i,n}\dot{W}'_{mn}(t)\dot{W}'_{in}(t)\sin\frac{m\pi\bar{x}}{a}\sin\frac{i\pi\bar{x}}{a}\,\mathrm{d}t. \tag{17}$$

The requirement $\Delta U_d = \Delta U'_d$ results in the expression for the damping coefficient of the wire. The hysteresis damping in the system of wires can subsequently be determined from (4).

It is worth mentioning that the area enclosed within the hysteresis loop and the associated damping depend on the loading rate (see for example, Gandi and Wolons, 1999). Accordingly, the damping coefficient derived using the approach shown in this section depends on the frequency of the applied dynamic load. While this is an interesting feature of the problem, according to the numerical examples shown below the effect of damping on the amplitude of forced vibration of the plate remains negligible as long as the driving frequency is close to or smaller than the fundamental frequency of the plate without SMA wires. In the contrary, the recovery forces in SMA wires have a profound influence on the amplitude of motion in this range of driving frequencies.

2.3. SMA wires in sleeves connected to the plate at discrete points

An alternative approach to design can employ SMA wires in the sleeves, or even without sleeves, connected to the plate at a number of points, rather than along a continuous line. For example, the concentrated force transmitted from the wire to the plate at the attachment points can be found for the cases shown in Figs. 5 and 6.

It is easily shown that the reaction of a wire attached at the mid-point (Fig. 5) and oriented in the x-direction is given by

$$R_{w1} \approx 4T\frac{w}{a}. \tag{18}$$

The forces transmitted to the plate by a wire attached at three symmetric points (Fig. 6) are

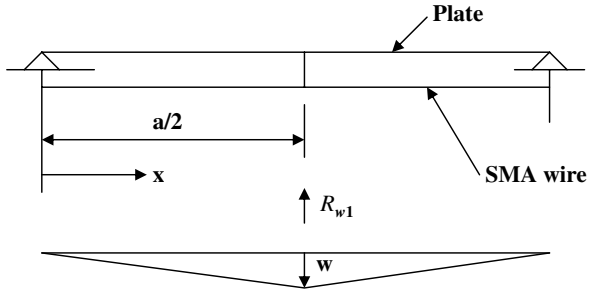

Fig. 5. Prestressed SMA wire connected to the plate at a single point. The lower figure illustrates a deformed shape of the wire (bending of wire is neglected due to prestress and a large difference between its natural frequency and the frequency of the driving load).

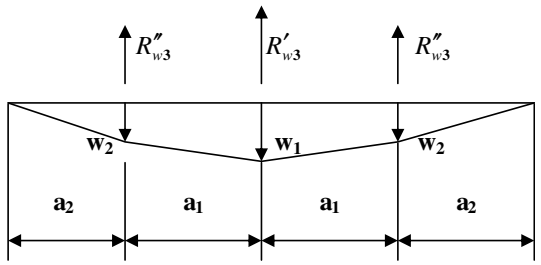

Fig. 6. Deformed shape of a SMA wire connected to the plate at three points.

$$R'_{w3} \approx 2T\frac{w_1 - w_2}{a_1}$$
$$R''_{w3} \approx T\left(\frac{w_2}{a_2} - \frac{w_1 - w_2}{a_1}\right). \tag{19}$$

Obviously, each force can be represented as a linear function of displacements of the points of connection of the wire to the plate. It is assumed that the wires are sufficiently stretched so that their bending between the points of connection to the plate during vibrations can be disregarded.

The elastic reactions of SMA wires can now be represented in terms of functions of deflections of the connection points, so that the reaction at a point (x_i, y_j) supported by wires in both x and y directions is

$$R_w(x_i, y_j, t) = a_{ij}w(x_i, y_j, t) + a_{(i-1)j}w(x_{i-1}, y_j, t) + a_{(i+1)j}w(x_{i+1}, y_j, t) + a_{i(j-1)}w(x_i, y_{j-1}, t) + a_{i(j+1)}w(x_i, y_{j+1}, t). \tag{20}$$

where the subscripts identify the points of wire connection to the plate and the coefficients a_{ij} are easily available.

Collecting the reactions of SMA wires at all connection points the overall reaction of the system of wires can be represented by

$$p_w = \sum_{i,j} k_{ij}w(x_i, y_j, t), \tag{21}$$

where k_{ij} are coefficients dependent on the prestress of wires and the location of the connection points.

The Galerkin procedure applied to the equations of motion yields the following coefficient at the corresponding term in (11):

$$K_{rsmn} = \frac{4}{ab}\sum_{r,s} k_{rs}S_{rm}(x_r)S_{sn}(y_s). \tag{22}$$

The energy dissipated due to damping in a SMA wire experiencing vibrations with the strain range equal to $2\Delta\varepsilon$ is evaluated as explained above (see (16)). The energy dissipated due to an equivalent viscous damping is determined using the velocities of the wires at the connection points. For example, for the wire oriented along $x = \bar{x}$ and connected at N points $x = \bar{x}$, $y = y_k$ ($k = 1, 2, \ldots N$) the energy dissipation due to an equivalent system of viscous damping elements at these points is calculated from

$$\Delta U'_{\mathrm{d}} = \frac{1}{2}\int_0^{2\pi/\omega}\int_0^b C'_{\mathrm{w}y}\delta(y-y_k)\dot{w}^2(\bar{x},y,t)\,\mathrm{d}y\,\mathrm{d}t$$
$$= \frac{1}{2}C'_{\mathrm{w}y}\sum_k\int_0^{2\pi/\omega}\sum_{m,n}\sum_{i,j}\dot{W}_{mn}(t)\dot{W}_{ij}(t)\,\sin\frac{m\pi\bar{x}}{a}\sin\frac{\mathrm{i}\pi\bar{x}}{a}\sin\frac{n\pi y_k}{b}\sin\frac{\mathrm{j}\pi y_k}{b}\,\mathrm{d}t. \tag{23}$$

Equating the energy dissipation given by (16) to that according to (23) it is possible to evaluate the equivalent viscous damping. The damping effect applied at all connection points can now be written in the form similar to (21), i.e.

$$p_{\mathrm{d}} = \sum_{i,j} c'_{ij}\dot{w}(x_i,y_j,t). \tag{24}$$

In (24), is c'_{ij} a damping coefficient accounting for the equivalent viscous damping produced by all wires connected to the plate at the point $x = x_i$, $y = y_j$.

The term reflecting viscous damping in equations of motion (11) becomes

$$C_{rsmn} = \frac{4}{ab}\sum_{r,s} c'_{rs}S_{rm}(x_r)S_{sn}(y_s). \tag{25}$$

The inertial terms in equations of motion must reflect the fact that wires are connected at a limited number of points (x_i, y_j). The corresponding contribution to rotational inertias can be neglected. If the mass of wires and sleeves at the point (x_i, y_j) is m_{ij}, the mass per unit surface area is

$$\bar{m}(x,y) = \rho_{\mathrm{p}}h + \sum_{i,j} m_{ij}\delta(x-x_i)\delta(y-y_j). \tag{26}$$

Accordingly, the corresponding coefficient in (11) is

$$M_{rsmn} = \rho_{\mathrm{p}}h + \frac{4}{ab}\sum_{i,j} m_{ij}S_{rm}(x_i)S_{sn}(y_j). \tag{27}$$

2.4. Thin plate supported by SMA wires

If the plate is thin all previous derivations concerning the stiffness and damping contributions of SMA remain unchanged. The equation of motion becomes

$$D_{11}w_{,xxxx} + 2(D_{12}+2D_{66})w_{,xxyy} + D_{22}w_{,yyyy} + m(x,y)\ddot{w} + [c_1(x)+c_2(y)]\dot{w} + [k_1(x,y)+k_2(x,y)]w = q(x,y,t). \tag{28}$$

The deflection represented by the first series (10) satisfies boundary conditions for a simply supported plate. Upon the substitution of the deflection into (28) and the application of the Galerkin procedure the equations of motion become

$$\sum_{r,s}\left[M_{rsmn}\ddot{W}_{rs} + C_{rsmn}\dot{W}_{rs} + K_{rsmn}W_{rs}\right] + F_{mn}W_{mn} = \sum_{rs} q_{rsmn}(t), \tag{29}$$

where the coefficients M_{rsmn}, C_{rsmn}, K_{rsmn} and $q_{rsmn}(t)$ are not altered compared to the case of a shear deformable plate. The coefficient reflecting the stiffness of the plate is

$$F_{mn} = D_{11}\left(\frac{m\pi}{a}\right)^4 + 2(D_{12}+2D_{66})\left(\frac{m\pi}{a}\right)^2\left(\frac{n\pi}{b}\right)^2 + D_{22}\left(\frac{n\pi}{b}\right)^4. \tag{30}$$

3. Numerical examples

The effectiveness of the proposed method was illustrated on the example of composite and isotropic plates supported at the center by two mutually perpendicular SMA wires, each of them parallel to a pair of plate edges. The load was represented by a harmonic pressure with the frequency close to the fundamental frequency of the plates without activated SMA wires. The plate considered in Figs. 7–9 was cross-ply symmetrically laminated and manufactured from AS/3501-6 graphite epoxy. The example in Fig. 10 is shown for an aluminum Al 2024 plate. The force in the wires was estimated based on the recovery stress of 220 MPa recorded by Cross for nitinol (Cross et al., 1970). For example, the recovery force in a 5-mm diameter wire would be equal to $T = 4.32$ kN. This estimate determined the range of recovery forces considered in the examples. The driving frequencies considered in the examples were in the vicinity of the fundamental frequency of the plate without SMA wires. As is shown in Section 3.1, the effect of hysteretic damping is negligible in this range of frequencies compared to that of the recovery force in SMA wires. Accordingly, the following results were generated without accounting for this effect, except for several representative cases that confirmed the validity of neglecting the effect of damping.

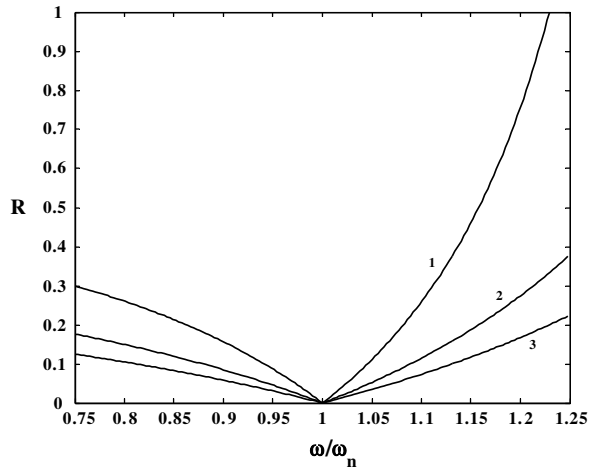

Fig. 7. Effect of SMA wires supporting the center on the amplitude of vibrations of a square AS/3501-6 plate ($a = b = 1.0$ m, $h = 4.0$ mm). Case 1: $T = 3.0$ kN, case 2: $T = 6.0$ kN, case 3: $T = 9.0$ kN.

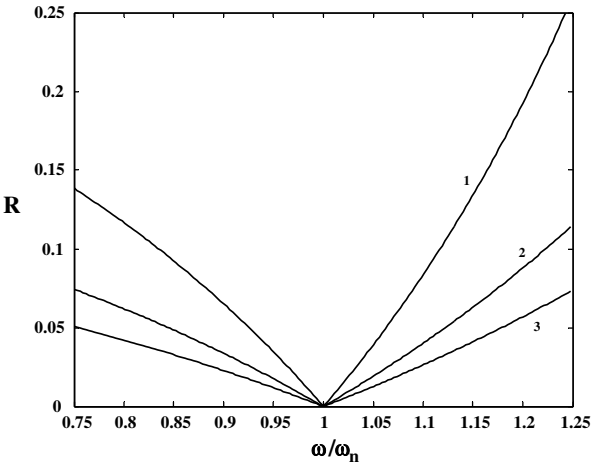

Fig. 8. Effect of SMA wires supporting the center on the amplitude of vibrations of a square AS/3501-6 plate ($a = b = 1.0$ m, $h = 2.0$ mm). Case 1: $T = 1.0$ kN, case 2: $T = 2.0$ kN, case 3: $T = 3.0$ kN.

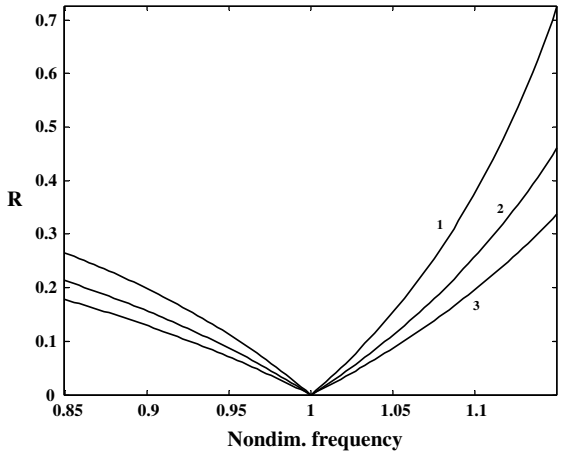

Fig. 9. Effect of the size on the amplitudes of vibrations of a 4-mm thick square AS/3501-6 plate supported at the center by SMA wires with the recovery force equal to 3 kN. Case 1: $a = b = 0.75$ m, case 2: $a = b = 1.0$ m, case 3: $a = b = 1.25$ m. The axis "Nondim. frequency" refers to the ratio ω/ω_n for the corresponding plate.

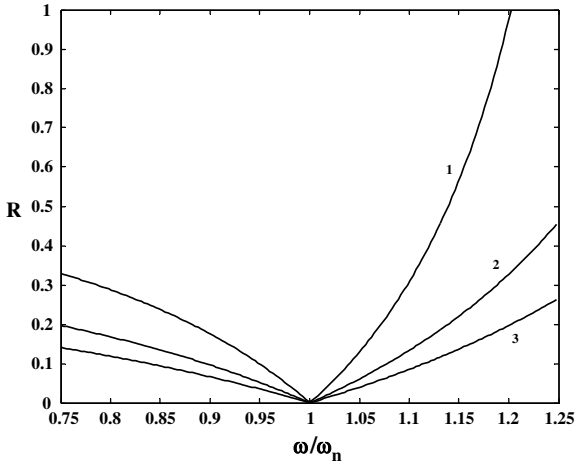

Fig. 10. Effect of SMA wires supporting the center on the amplitude of vibrations of a square aluminum (Al 2024) plate ($a = b = 1.0$ m, $h = 4.0$ mm). Case 1: $T = 2.0$ kN, case 2: $T = 4.0$ kN, case 3: $T = 6.0$ kN.

The following figures illustrate relationships between the nondimensional frequency (ω/ω_n) calculated as a ratio of the driving frequency to the fundamental frequency of the plate without wires and a reduction in the amplitude of motion, i.e. the ratio of the amplitude of the plate with SMA wires to the amplitude of the same plate without such wires (R). As follows from Figs. 7 and 8, it is possible to significantly reduce the amplitude of motion of AS/3501-6 plates using SMA wires that support them at the center. The maximum reduction was achieved at the fundamental frequency. At lower driving frequencies the effectiveness of the method was reduced but it was still significant, even when the driving frequency was equal to 75% of the fundamental frequency value. At higher driving frequencies the presence of SMA wires that support the center of the plate becomes counterproductive due to the resonance in the plate–wire system whose fundamental frequency is higher than that in the plate without wires. Accordingly, the proposed method is effective only if the driving frequencies remain close to or smaller than the fundamental frequency of the plate without activated SMA wires. Predictably, a larger recovery force in SMA wires increases their effect on the amplitude of vibrations. Thinner plates (Fig. 8) are more affected by the presence of wires than thicker and stiffer counterparts (Fig. 7), even though the recovery force generated in the wires supporting the former plates was smaller.

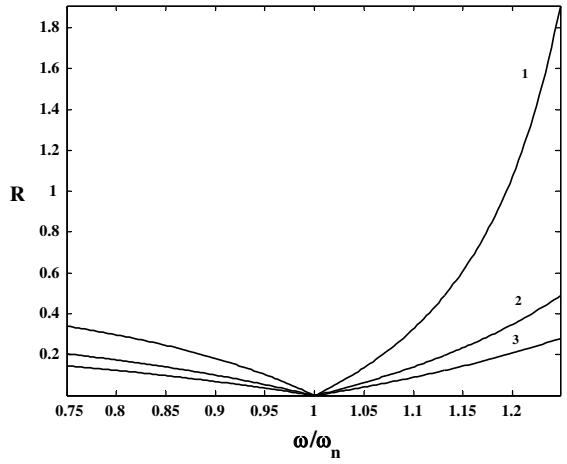

Fig. 11. Effect of SMA wires providing continuous support on the amplitude of vibrations of an aluminum (Al 2024) beam ($a = 1.0$ m, $h = 3.0$ mm, $b/l_y = 2$). Case 1: $T = 0.5$ kN, case 2: $T = 1.0$ kN, case 3: $T = 1.5$ kN.

The effect of the size of the plate on the effectiveness of SMA wires is depicted in Fig. 9. Predictably, larger plates that have a lower stiffness are affected by SMA wires to a larger degree than their otherwise identical but smaller counterparts. Finally, the results for aluminum plates shown in Fig. 10 confirm all conclusions previously discussed in regard to Figs. 7 and 8.

The effect of SMA wires embedded in sleeves that are oriented in the x-direction and continuously bonded to a large aspect ratio plate with simply supported short edges and free long edges (essentially, a beam) is shown in Fig. 11. As follows from this figure, a continuous elastic support provided by SMA wires can be as effective as the concentrated resisting force considered in the previous examples significantly reducing the amplitude of forced vibrations.

While the previous examples clearly illustrate the benefits of two methods of passive vibration control considered in the paper, it is necessary to estimate the additional weight added to the structure as a result of using SMA wires. The weight of sleeves can be assumed negligible compared to that of wires, i.e. it is sufficient to compare the weight of SMA wires necessary to develop prescribed tensile forces to the weight of the supported structure. For example, the weight of SMA wires necessary to develop the tensile force $T = 4.32$ kN in the plates considered in Fig. 7 represents about 5% of the weight of the plate. In the example considered in Fig. 11, the weight of SMA wires necessary to develop the force $T = 1.5$ kN was equal to 5.4% of the weight of the structure. These estimates illustrate that it is possible to control forced vibrations of composite and isotropic plates and beams using SMA wires that add only a small fraction to the overall weight of the structure.

3.1. Estimate of the contribution of hysteretic damping to a reduction of the amplitude of forced vibration

It is instructive to estimate the contribution of damping to a reduction of the amplitude of motion depicted in Figs. 7–11. The loss of energy in Nitinol wires was considered in the paper of Gandi and Wolons (1999) for various frequencies of vibration and temperatures. As follows from the results shown in this paper, the damping ratio of the superelastic Nitinol increases with a decrease in the frequency of motion. Furthermore, damping decreases with a larger static offset (static prestress). A higher temperature also contributed to a decrease in damping. Consider for example the estimate of damping based on data from Fig. 13 of the above-mentioned paper for the case of the driving frequency equal to 4 Hz (room temperature, strain range of 3.93%). The loss factor corresponding to a complete hysteresis loop obtained as a ratio of the loss modulus to the storage modulus was approximately equal to $\eta = 2.5 \times 10^5$ psi/13.0×10^6 psi $= 0.192$. However, as explained bellow, such loss factor cannot be attained in the configurations considered in the paper since the actual strain range is limited by the allowable strain in the plate material.

In the first approximation, a plate vibrating in the vicinity of the fundamental frequency can be analyzed as a single degree of freedom system. In the presence of hysteretic damping, the motion of such system is characterized by Nashif et al. (1985):

$$m'\ddot{w}' + k'(1 + i\eta')w' = \mathrm{Re}\left[F e^{i\omega t}\right], \tag{31}$$

where the terms with the prime identify the mass, stiffness, displacement and loss factor (prime is used to distinguish these terms from the notation in the previous part of the paper) and the term in the right side represents the driving force.

The motion of the system described by (31) is immediately available, the amplitude being equal to

$$W' = \frac{F}{\sqrt{(k' - m'\omega^2)^2 + k'^2\eta'^2}}. \tag{32}$$

The reduction factor representing a ratio of the amplitude of motion with hysteretic damping to that without such damping is given by

$$R_\mathrm{d} = \sqrt{\frac{\left[1 - \left(\omega/\omega_n'\right)^2\right]^2}{\left[1 - \left(\omega/\omega_n'\right)^2\right]^2 + \eta'^2}}, \tag{33}$$

where ω_n' is the fundamental frequency of the system with activated SMA wires.

Note that the loss factor in (31)–(33) is different from the factor evaluated above since it must account for the cross sectional area and number of SMA wires. In the first-approximation quantitative analysis one can assume that SMA wires are smeared over the surface of the plate so that their damping is incorporated in the properties of the plate material. This implies that $\eta' = V_\mathrm{w}\eta$ where V_w is a ratio of the volume of SMA wires to the volume of the plate.

It is obvious that in efficient applications the ratio V_w should be small. As indicated above, the desirable effect of the recovery stress in SMA wires could be achieved when their weight was of an order of 5% of the weight of the plate. Hence it may conservatively be assumed that the volume of SMA wires will not exceed 10% the plate volume, i.e. $V_\mathrm{w} \leqslant 0.1$. The frequency ratio in (33) can be estimated considering the stiffening of the plate produced by the recovery forces in the wires that effectively "shifts" the fundamental frequency to larger values as reflected in Figs. 7–11. It is estimated that such "shift" was no less than 20% (a slightly smaller shift is possible in case 1 in Fig. 10). Hence if the driving frequency is equal to the fundamental frequency of the plate without SMA wires, the ratio $\omega/\omega_n' \leqslant 0.83$.

It remains to estimate the actual loss factor corresponding to the incomplete hysteresis loop as against the factor for the complete loop. The range of strain allowable for both cross ply graphite/epoxy and Al 2024 plates considered in the examples is under 1%. At such limited range of strains, the discrepancy between the loss factors for various strain rates becomes small (see Fig. 7 in the paper by Gandi and Wolons, 1999). Moreover, the value of the loss factor decreases compared to that for a large range of strain. For example, if the amplitude of strain is about 0.5%, the extrapolation of data in Fig. 7 of the above-mentioned paper yields the loss factor that is approximately equal to 0.12. Using this value in (33) with $V_\mathrm{w} = 0.1$ one obtains the reduction factor equal to 0.999. Hence if a plate driven at its fundamental frequency vibrates with the strain amplitude approaching 0.5%, the effect of hysteretic damping is negligible. The hysteretic damping becomes even less important at smaller frequencies but its effect increases at higher frequencies. Obviously, this effect dominates when $\omega/\omega_n' \to 1.0$.

4. Conclusions

The paper presents a methodology of the dynamic analysis of composite and isotropic plates supported by SMA wires. The solution is obtained for shear deformable plates using the first-order theory and for thin plates by the classical plate theory. Two designs of SMA reinforcements are considered, including wires in sleeves that are continuously bonded to the surface of the plate and wires attached to the plate at selected

points. In the first method, the spacing of wires can be nonuniform to achieve the maximum effectiveness using the prescribed amount of SMA. Similarly, in the second case, the points of attachment of SMA wires to the plate can be chosen to maximize their effect.

SMA wires considered in the paper are prestressed through the phase transformation. It is assumed that they operate in the austenitic phase. Accordingly, SMA wires reduce the amplitude of forced vibrations through two mechanisms: (1) they resist deflections of the structure acting similar to an elastic foundation and (2) dissipation of energy in the wires occurs as a result of the hysteresis. The former mechanism dominates when the driving frequency is close to or smaller than the fundamental frequency of the plate determined without accounting for the effect of SMA wires, while hysteretic damping becomes important at higher driving frequencies approaching the resonant value for the plate with prestressed SMA wires.

Numerical examples presented in the paper confirm that SMA wires supporting composite and isotropic plates can serve as an effective tool for passive vibration control. The wires effectively "shift" the resonance frequencies of the plate to larger values. Therefore, they should be used selectively, only in applications where the spectrum of driving frequencies is known in advance.

Acknowledgements

This research was supported by the Army Research Office, Contract W911NF-06-1-0189. The program mangers were Drs. Bruce LaMattina and Gary L. Anderson.

Appendix. Effect of prestressed SMA wires on the amplitude of forced vibrations of a composite or isotropic beam

The study by Epps and Chandra (1997) illustrated that SMA wires can increase the natural frequencies of a composite beam. This Appendix provides an approximate formula that predicts the effect of such wires on the amplitude of forced vibration that occur in the frequency range where it is possible to neglect hysteretic damping.

Consider a large aspect ratio plate or a slender beam supported by a system of SMA wires oriented along the long edges of the plate or along the beam axis (see Fig. 1 where $a \gg b$). The plate (beam) subject to a uniform harmonic pressure per unit length $p = p\sin\omega t$ is simply supported at $x = 0$ and a and free along $y = 0$ and b. The approximate solution is obtained by the Rayleigh–Ritz method assuming the mode shape of motion in the form

$$w = \frac{4W(t)(a-x)x}{a^2}. \tag{A1}$$

Expression (A1) satisfies kinematic boundary conditions. The static conditions are violated but this is acceptable using the Rayleigh–Ritz method.

The strain energy of the elastic foundation provided by a system of SMA wires is

$$U_{\mathrm{w}} = \frac{b}{2}\int_0^a k_2 w^2\,\mathrm{d}x = \frac{4Tb}{3l_y a}W^2. \tag{A2}$$

The strain and kinetic energies of the vibrating plate (beam) are

$$\begin{aligned} U_{\mathrm{b}} &= \frac{b}{2}\int_0^a D_{11}\left(\frac{\mathrm{d}^2 w}{\mathrm{d}x^2}\right)^2\mathrm{d}x = 32D_{11}\frac{b}{a^3}W^2 \\ K &= \frac{1}{2}\int_0^a m\dot{w}^2\,\mathrm{d}x = \frac{4}{15}ma\dot{W}^2, \end{aligned} \tag{A3}$$

respectively, where m is the mass per unit length.

The work of the applied pressure is found as

$$U_{\mathrm{p}} = \int_0^a pw\,\mathrm{d}x = \frac{2}{3}paW. \tag{A4}$$

The Lagrange equation yields the following equation of motion:

$$\frac{8}{15}ma\ddot{W}+\frac{8}{3}\frac{T}{a}\frac{b}{l_y}W+64D\frac{b}{a^3}W=\frac{2}{3}pa. \tag{A5}$$

In the absence of SMA wires the natural frequency found from (A5) is 11% higher than that available from the exact solution. Therefore, representing the motion in the form (A1) is adequate for a qualitative analysis only.

Characterizing the forced response by $W=\widetilde{W}\sin\omega t$, the amplitude of motion found from (A5) is obtained as

$$\widetilde{W}=\frac{2pa/3}{-8ma\omega^2/15+8Tb/3al_y+64D_{11}b/a^3}. \tag{A6}$$

The ratio of the amplitude of forced vibrations with the SMA effect to that without such effect can be presented in the form

$$R=\frac{1-\bar{\omega}^2}{1-\bar{\omega}^2+Ta^3/24D_{11}l_y^2}, \tag{A7}$$

where $\bar{\omega}=\omega/\omega_n$. Note that it is implicitly assumed in (A7) that the effect of SMA wires and sleeves on the mass of the structure is negligible.

References

Baz, A., Poh, J., Ro, J., Gilheany, J., 1995. Control of the natural frequencies of nitinol-reinforced composite beams. Journal of Sound and Vibrations 185, 171–185.

Birman, V., 1997a. Review of mechanics of shape memory alloy structures. Applied Mechanics Reviews 50, 629–645.

Birman, V., 1997b. Theory and comparison of the effect of composite and shape memory alloy stiffeners on stability of composite shells and plates. International Journal of Mechanical Sciences 39, 1139–1149.

Cross, W.B, Kariotis, A.H., Stimler, FJ., 1970. Nitinol characterization study. NASA CR-1433.

Epps, J., Chandra, R., 1997. Shape memory alloy actuation for active tuning of composite beams. Smart Materials and Structures 6, 251–264.

Gandi, F., Wolons, D., 1999. Characterization of the pseudoelastic damping behavior of shape memory alloy wires using complex modulus. Smart Materials and Structures 8, 49–56.

Ip, K.-H., 2000. Energy dissipation in shape memory alloy wires under cyclic bending. Smart Materials and Structures 9, 653–659.

Lagoudas, D.C., Khan, M.M., Mayes, J.J., Henderson, B.K., 2004. Pseudoelastic SMA spring elements for passive vibration isolation. Part II: Simulation and experimental correlations. Journal of Intelligent Material Systems and Structures 15, 443–470.

Masuda, A., Noori, M., 2002. Optimization of hysteresis characteristics of damping devices based on pseudoelastic shape memory alloys. International Journal of Non-Linear Mechanics 37, 1375–1386.

Nashif, A.D., Jones, D.I.G., Henderson, J.P., 1985. Vibration Damping. John Wiley and Sons, New York.

Reddy, J.N., 2004. Mechanics of laminated composite plates and shells. Theory and analysis. CRC Press, Boca Raton.

Ro, J., Baz, A., 1995. Nitinol-reinforced plates: Part III. Dynamic characteristics. Composites Engineering 5, 91–106.

Saadat, S., Salichs, J., Noori, M., Hou, Z., Davoodi, H., Bar-On, I., Suzuki, Y., Masuda, A., 2002. An overview of vibration and seismic applications of NiTi shape memory alloy. Smart Materials and Structures 11, 218–229.

Seelecke, S., Heintze, O., Masuda, A., 2002. Simulation of earthquake-induced structural vibrations in systems with SMA damping elements. In: Proceedings of the SPIE Smart Structures and Materials Conference, vol. 4697, pp. 238–245.

Soedel, W., 1993. Vibrations of Shells and Plates. Marcel Dekker, New York.

Thomson, P., Balas, G.J., Leo, P.H., 1995. The use of shape memory alloy for passive structural damping. Smart Materials and Structures 4, 36–42.

Zak, A.J., Cartmell, M.P., Ostachowicz, W.M., Wiercigroch, M., 2003. One-dimensional shape memory alloy models for use with reinforced composite structures. Smart Materials and Structures 12, 338–346.

Zhang, W., Kim, J., Koratkar, N., 2003. Energy-absorbent composites featuring embedded shape memory alloys. Smart Materials and Structures 12, 642–646.